ARMY RESEARCH LABORATORY

An Experimental Method for Dynamic Properties of Composites at Interior Ballistic Rates of Loading

Jerome T. Tzeng
Ara S. Abrahamian

ARL-TR-696

February 1995

NOTICES

REPORT DOCUMENTATION PAGE	Form Approved OMB No. 0704-0188

1. AGENCY USE ONLY *(Leave blank)*	2. REPORT DATE	3. REPORT TYPE AND DATES COVERED
	February 1995	Final, October 1992 - October 1993

4. TITLE AND SUBTITLE

An Experimental Method for Dynamic Properties of Composites at Interior Ballistic Rates of Loading

5. FUNDING NUMBERS

PR: 1L162618AH80

6. AUTHOR(S)

Jerome T. Tzeng and Ara S. Abrahamian

7. PERFORMING ORGANIZATION NAME(S) AND ADDRESS(ES)

U.S. Army Research Laboratory
ATTN: AMSRL-WT-TD
Aberdeen Proving Ground, MD 21005-5066

8. PERFORMING ORGANIZATION REPORT NUMBER

9. SPONSORING/MONITORING AGENCY NAME(S) AND ADDRESS(ES)

U.S. Army Research Laboratory
ATTN: AMSRL-OP-AP-L
Aberdeen Proving Ground, MD 21005-5066

10. SPONSORING/MONITORING AGENCY REPORT NUMBER

ARL-TR-696

11. SUPPLEMENTARY NOTES

12a. DISTRIBUTION/AVAILABILITY STATEMENT

Approved for public release; distribution is unlimited.

12b. DISTRIBUTION CODE

13. ABSTRACT *(Maximum 200 words)*

An experimental method that uses an airgun system was developed to investigate the dynamic response of materials in a gun launch environment. An energy-absorbing test fixture was designed to generate the desired loading conditions in the specimen as it decelerated the gun-launched projectile. Methods of data acquisition and reduction were developed using a streak camera and a film digitization technique. The system was calibrated and verified by testing aluminum samples, and fairly good results were obtained. The technique was then applied to a polymer composite laminate having a particular layup construction of interest. Strain rate effects on the compressive strength were observed at the interior ballistic rates of loading.

14. SUBJECT TERMS	15. NUMBER OF PAGES
composite materials, dynamic property, interior ballistics, high strain rate, air guns	27
	16. PRICE CODE

17. SECURITY CLASSIFICATION OF REPORT	18. SECURITY CLASSIFICATION OF THIS PAGE	19. SECURITY CLASSIFICATION OF ABSTRACT	20. LIMITATION OF ABSTRACT
UNCLASSIFIED	UNCLASSIFIED	UNCLASSIFIED	UL

NSN 7540-01-280-5500

Standard Form 298 (Rev. 2-89)
Prescribed by ANSI Std Z39-18
298-102

INTENTIONALLY LEFT BLANK.

ACKNOWLEDGMENTS

This report was prepared for a FY93 CURE program "Dynamic Behavior of Materials at Interior Ballistic Rates of Loading," which was supported by Dr. John Frasier, U.S. Army Research Laboratory (ARL). The authors would like to express their gratitude to Mr. William Mcintosh, ARL, for his engineering support and Dr. William Drysdale, ARL, for his helpful discussion.

INTENTIONALLY LEFT BLANK.

TABLE OF CONTENTS

INTENTIONALLY LEFT BLANK.

LIST OF FIGURES

INTENTIONALLY LEFT BLANK.

1. INTRODUCTION

Dynamic behavior of materials is characterized using standard testing machines for strain rates up to 10 s^{-1}, and in Hopkinson Bar experiments at strain rates greater than 100 s^{-1} (Kolsky 1949; Nicholas and Bless 1985; Staab and Gilat 1991). This generally leaves a gap in the measure of strain rates effects in the 10–100 s^{-1} band, precisely the zone of interest for launching of projectiles. The nominal strain rate in most of these current tests is held constant until failure of the specimen. While this procedure does give a good picture of the increase of yield and ultimate stress, with increasing strain rate for rate-sensitive materials, it is unclear whether the observed increase in strength at failure can be effectively used to prevent failure of materials subjected to short, high-rate, impulsive loads experienced during the interior ballistic cycle.

For fiber-reinforced polymer composites, the matrix-dominated properties, such as shear and transverse tensile strength, in general, increase with strain rate. Fibers such as graphite and glass are not rate-sensitive materials; however, the fiber-dominated properties may also increase due to the effects of the strengthening matrix. This is especially true for compressive properties, since a rigid and strong matrix may provide better lateral supports to the fibers and enhance the strength of material.

For ballistic applications, the dynamic compressive strength is the most important property, but it also is difficult to determine. This report investigates the rate effects on the compressive properties of composites subjected to a gun pressure-type loading condition. An experimental method and testing procedure was developed to simulate the loading conditions experienced by artillery projectiles during launch from a tank cannon. These tests were intended to match the conditions observed for newer, higher performance guns. The systems were calibrated in tests of aluminum and demonstrated for the material of interest in the current effort—fiber-reinforced plastic.

2. EXPERIMENTAL CONFIGURATION

An airgun system with a designed test fixture and a data acquisition system is used to generate a ballistic-type loading condition in a specimen. The airgun system consists of a series of various diameter tubes (3, 4, and 7 in) and lengths. Figure 1 shows an overall layout of the airgun system. The breech area of the gun is located on the right-hand side where a projectile is loaded. The gun barrel is then evacuated to 1 torr and the projectile is released. The projectile is accelerated by atmospheric pressure

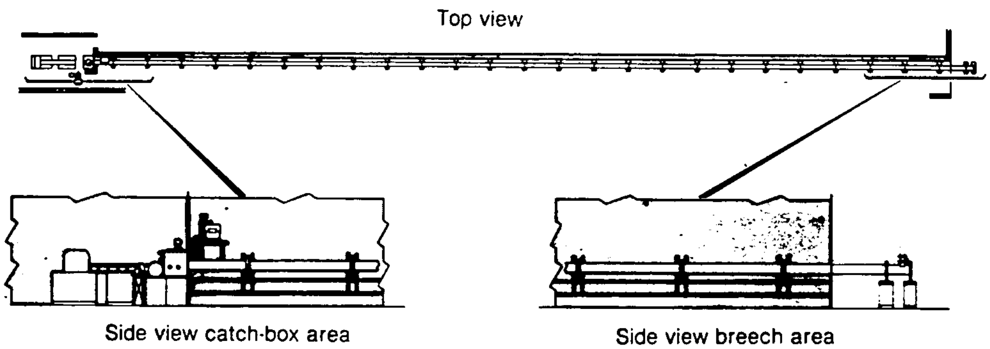

Figure 1. An overview of the airgun system.

(or slightly augmented) and travels for several hundred feet (up to 300 ft for the 7-in gun), achieving its terminal velocity in the catchbox area. In general, the size of the airgun selected is based on the energy level required for impact tests.

After muzzle exit, the projectile impacts a mitigator that is fabricated from honeycomb material and can be geometrically tailored for specific loading rates. Figure 2 illustrates the schematic of the impact testing setup. The momentum exchange mass (MEM) is a piece of heavy steel used to absorb the residual energy from impact. In general, the velocity of projectile, geometry of mitigator, and the mass of MEM are all selectable. By careful engineering of these features, the interior ballistic loading rates, pulse shapes, and durations can be realistically recreated during the deceleration of the projectile.

Using the above concept, the testing setup is designed and fabricated as shown in Figure 3. The specimen is held by a fixture between the mitigator and the MEM; therefore, an extra mass may be added in front of the fixture to adjust the force applied on the specimen. Fixtures are designed to hold the specimen in correct alignment during impact and provide uniform stress transfer into the specimen. The specimen can be flat or wedge shaped. The gauge length is adjustable, and test results can be compared to those collected using commercially available mechanical test fixtures such as Illinois Institute of Technology Research Institute (IITRI) or Celanese configurations by the American Society for Testing and Materials (ASTM) Standard D 3410 (Adams and Odom 1991; Adams and Lewis 1991). A 0.5-in gauge length is currently used for most investigations.

EXPERIMENTAL CONFIGURATION

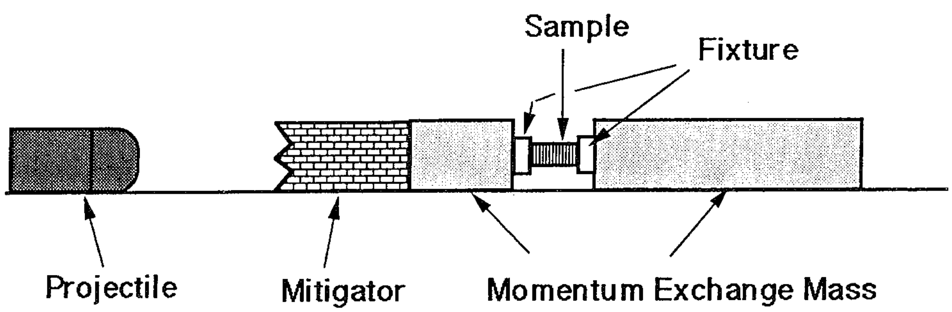

Figure 2. Schematic of experimental setup.

3. METHOD OF DATA ACQUISITION AND REDUCTION

Data acquisition methods were developed to determine both strain and stress measures in the sample during the impact event. Reliable and repeatable data were obtained, indicating the reliability of this newly developed system. Aluminum (6061-T6) samples (0.1 in thick and 1 in wide) were tested to calibrate the system. The 6061-T6 aluminum was selected because it is not rate-sensitive material, at least at the rate of our interest. Therefore, the airgun test results (at various strain rates) can be compared to the data measured at constant strain rate by Maiden and Green (1966).

3.1 Deformation. Measurements of displacements and deformations were collected via a streak camera. A strip pattern, shown in Figure 4a, is printed on the surface of the specimen. A high-speed camera photographed the strip during the impact event, and is activated by a sensor placed at the end of the gun tube. The speed of the camera is adjustable to cover the various durations of impact. Figure 4b shows a part of the streak film taken from an aluminum test at a film speed of 120 ft/s.

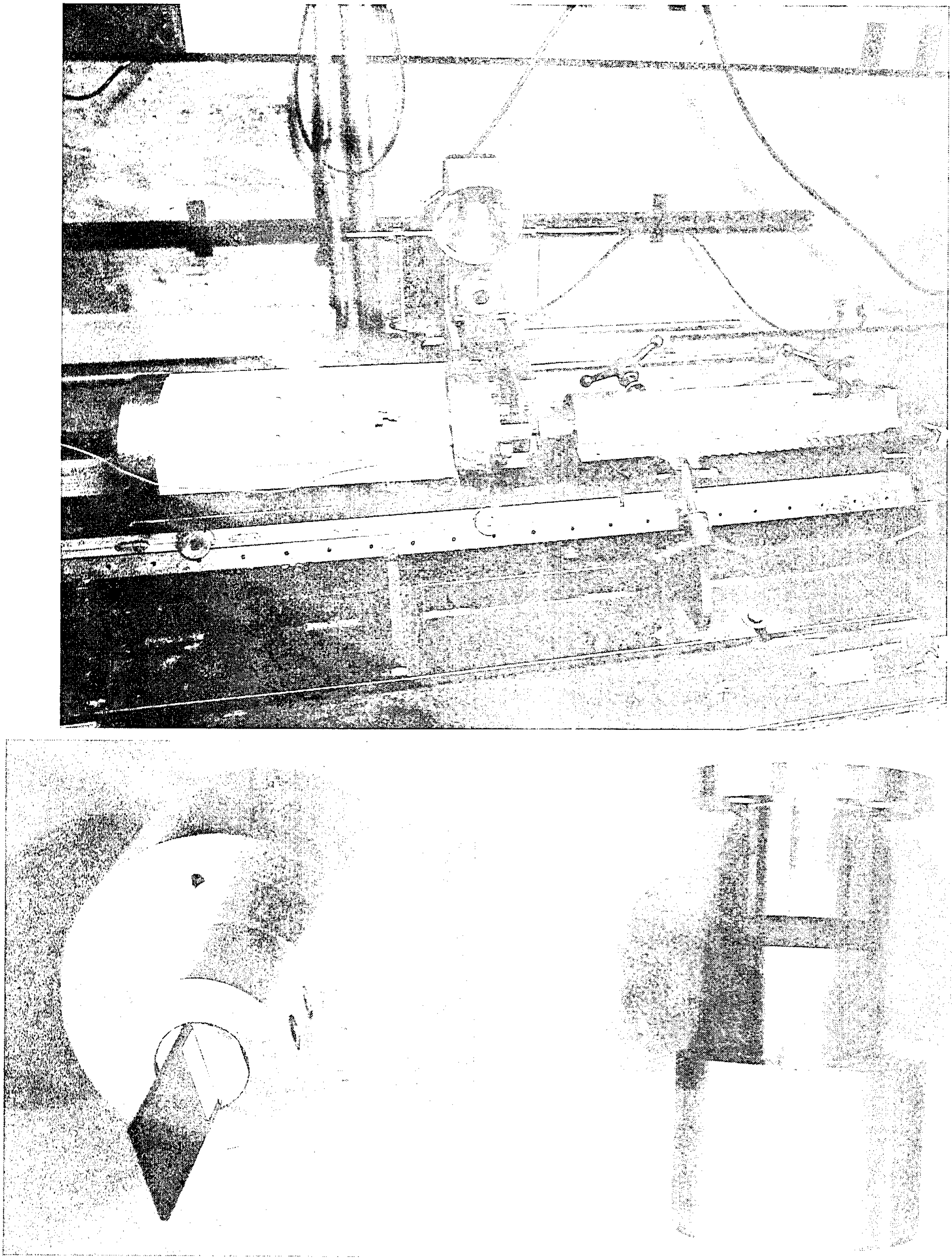

Figure 3. Testing setup and fixture with specimen.

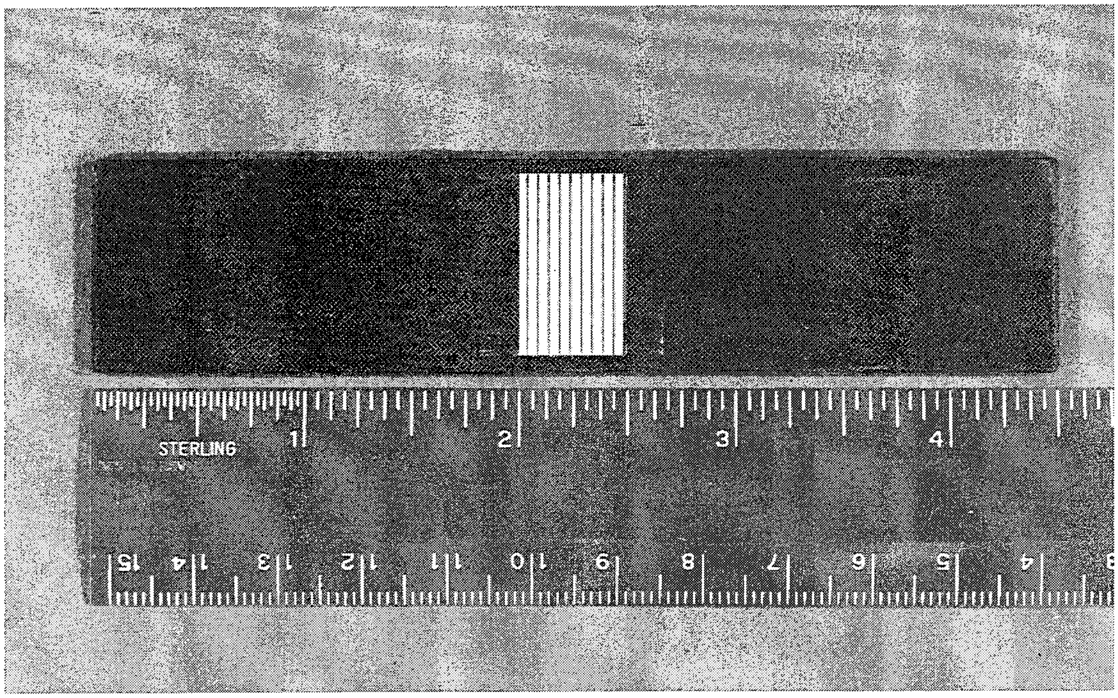

Figure 4a. Grid pattern on specimen surface.

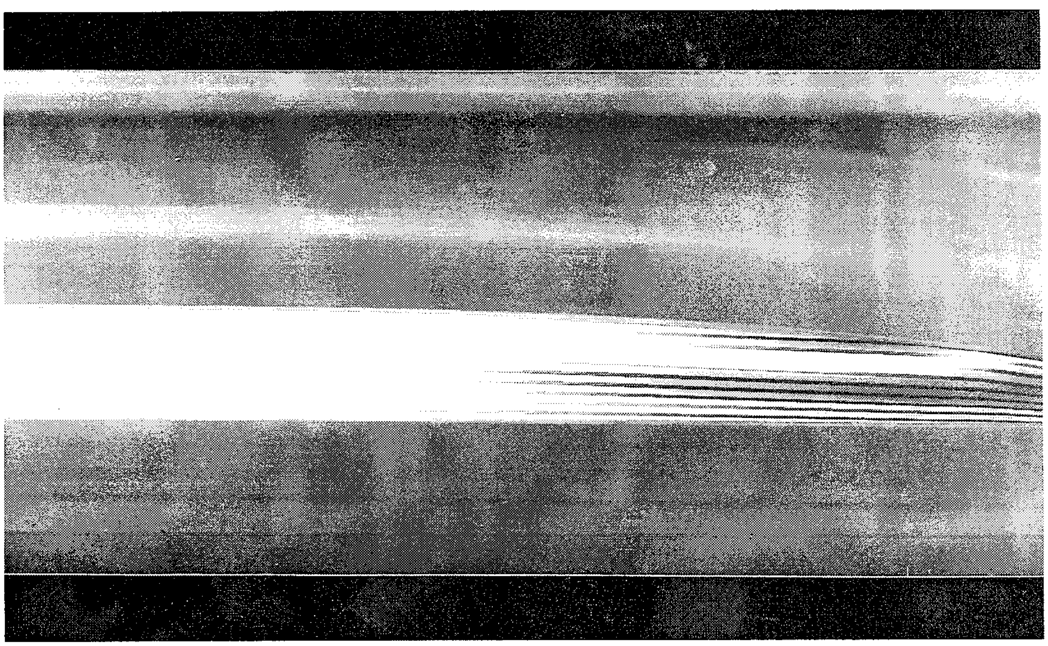

Figure 4b. Streak film taken from an aluminum test.

The parallel white/black strip on the film is the image of the strip pattern. It records both rigid body motion and deformation of the specimen as a function of time (along the length of film). The overall movement of the strip represents rigid body motion of the specimen, while the contraction of the strip corresponds to the compressive deformation due to impact. The streak film was then analyzed using a high-resolution PDS I0I0A microdensitometer and a PDS 2300C data acquisition system. The streak film is illuminated and light is received from the other side of the film. The received light is then digitized and expressed in terms of light density.

Figure 5 presents the light density scans at four time instants (the four corner plots) from one of the aluminum tests. As the material deformation increases, the distance between light intensity peaks decreases. The horizontal axis represents the position along the gauge length which is equally divided into about 5,000 spaces (over 0.5 in wide). Accordingly, the accuracy of the measurement is about 1×10^{-4} in or 0.02% of strain. A computer code was written to read this information and to identify the midpoint of each "valley" and "peak." The deformation can then be determined from the shifting of these valleys and peaks. Accordingly, the strain can be calculated and presented as a function illustrated in terms of impact time in the centerplot in Figure 5. The aluminum sample yielded at a strain of approximately 1% and failed at approximately 12% strain. The large deformation of the aluminum can clearly be observed in the streak film.

3.2 Force Measurement. An accelerometer was placed on the MEM surface to record the acceleration as a function in terms of impact time. The force in the specimen is assumed to be equal to the force acting on the MEM. Therefore, stress in the specimen can be derived and is equal to the product of the acceleration and the combined mass of MEM and the real part of the fixture. Accordingly, it is conservative in determination of the strength of material from this measured force.

Figure 6a illustrates the stress state in the sample attributable to impact. The curve with stress oscillation is the raw data measured by an accelerometer. This curve contains stress attributable to rigid body acceleration (acceleration of the whole system) and shock wave resulting from impact. To separate these two sources, a Fourier transform analysis (1991) is applied to decompose the frequency of the raw data shown in Figure 6b. Two major modes, one at 0 Hz and the other at about 5,500 Hz, were defined. The 0 Hz is attributable to rigid body acceleration, while the 5,500 Hz is resulting from acoustic waves. The period of acoustic wave traveling in the MEM is calculated to be 0.18 ms, which yields to a

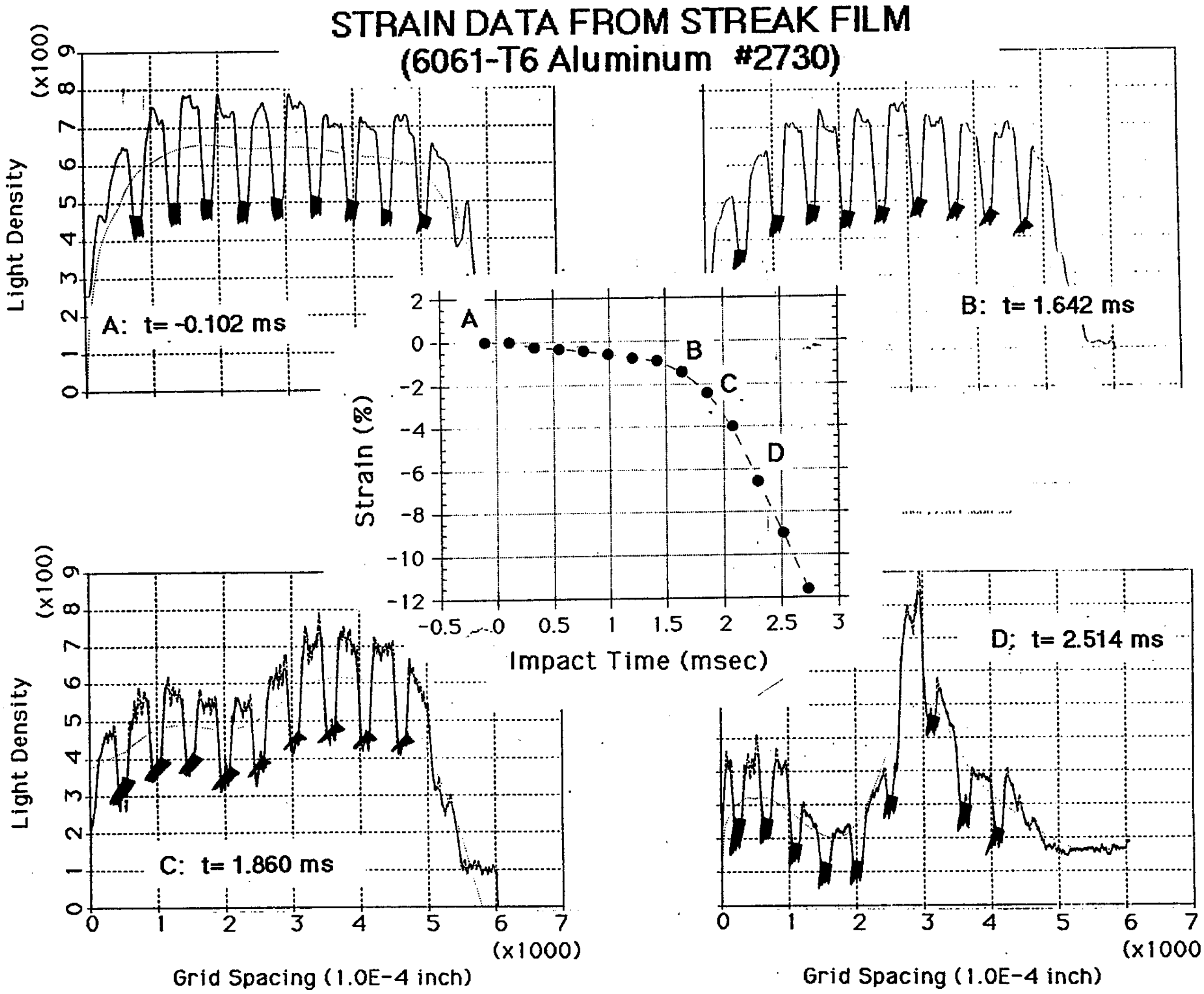

Figure 5. Strain field resulting from film analysis of aluminum test at four time instants.

frequency of about 5,500 Hz. The high-frequency (above 1,000 Hz) data is then culled from the raw data, resulting in a smooth master curve which contains rigid body acceleration only (Figure 6a).

Both stress and strain are obtained in terms of impact time and are compared to results measured by Maiden and Green (1966). As shown in Figure 7, fairly good agreement was obtained. The consistency of experimental results and good agreement to other test methods indicate the reliability and accuracy of this new testing system.

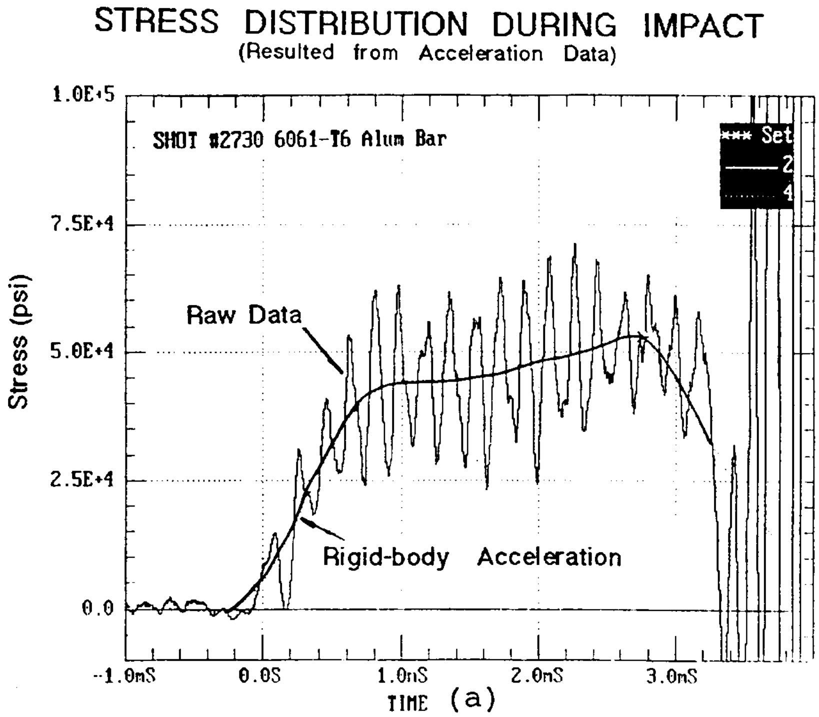

Figure 6a. Stress field resulting from acceleration data.

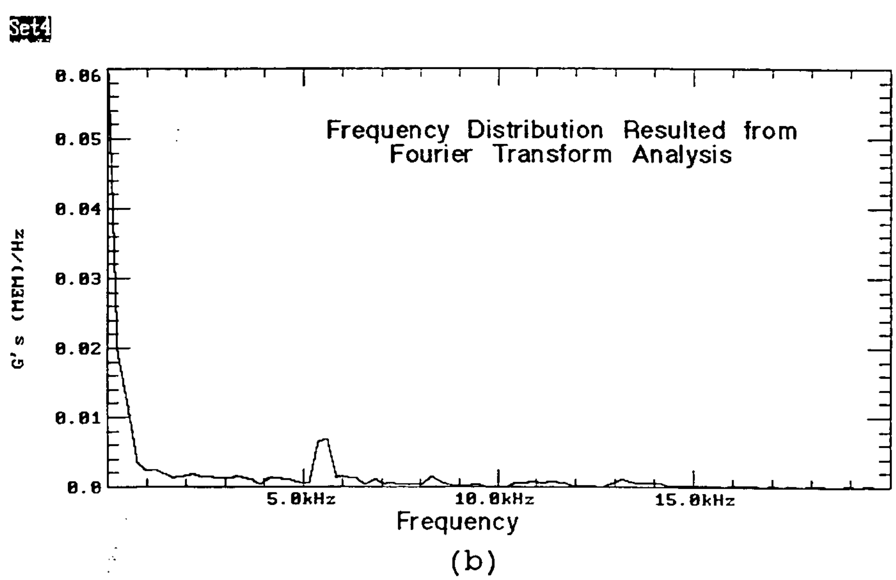

Figure 6b. Fourier transform analysis of raw data.

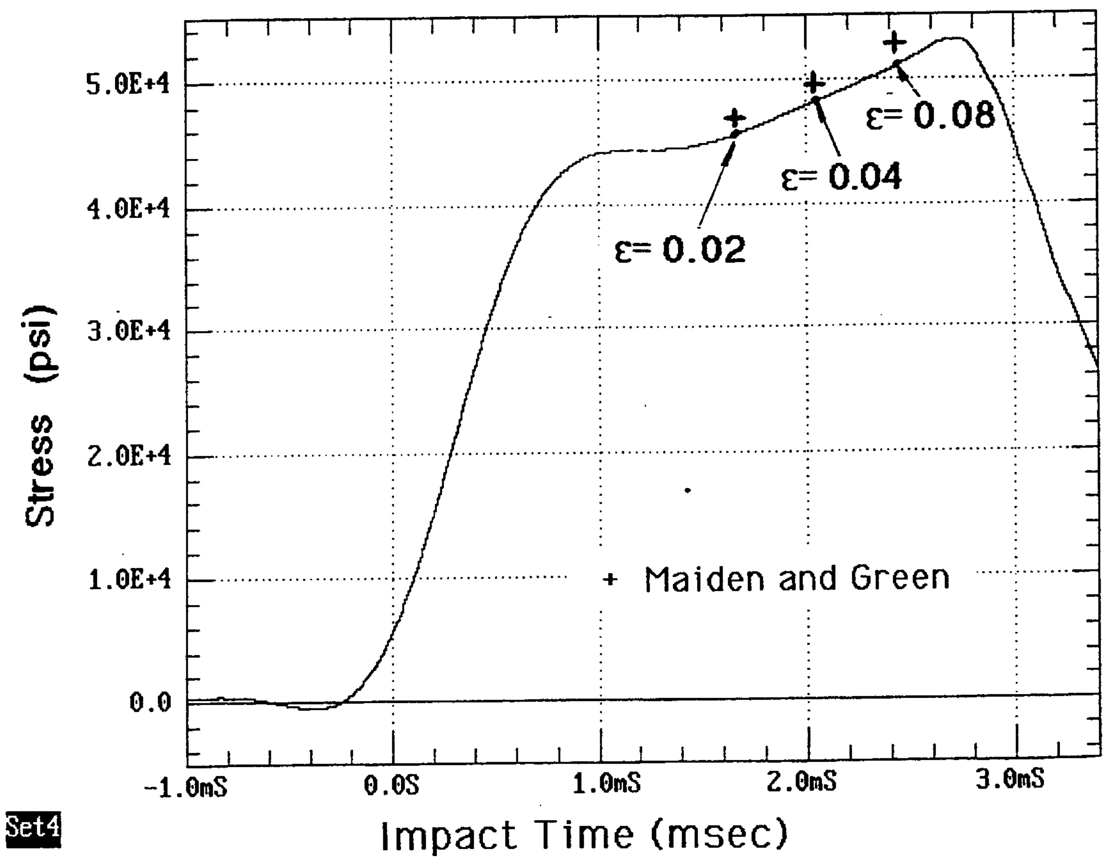

Figure 7. Comparison to the results measured by Maiden and Green (1966).

4. COMPOSITE RESULTS

The composite test coupon is also 1.00 in wide and 0.09 in thick with a layup construction of $[(0/45/-45/0)_4]$. Sixteen plies of Im7-graphite/8,551-7 epoxy composite laminates are fabricated using hot-pressed processes. The 0° plies have fibers oriented along the loading direction. The laminate has a balanced layup; therefore, no shear deformation is induced due to in-plane compression. The gauge length is 0.5 in, which prevents an early failure by buckling. More than 20 tests have been shot at various loading rates. The same procedure described in the aluminum test is used for all composite tests.

The streak film and strain in terms as a function of time from impact are illustrated in Figures 8a and 8b, respectively. A very sharp drop, significantly different from that seen for the aluminum test

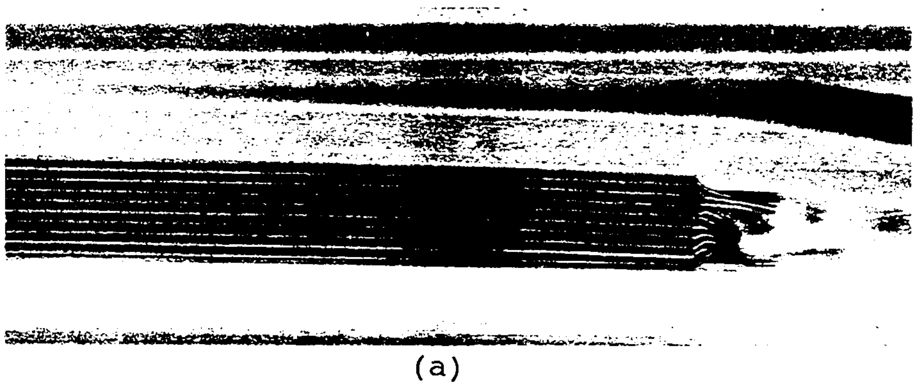

Figure 8a. Streak film resulting from composite test.

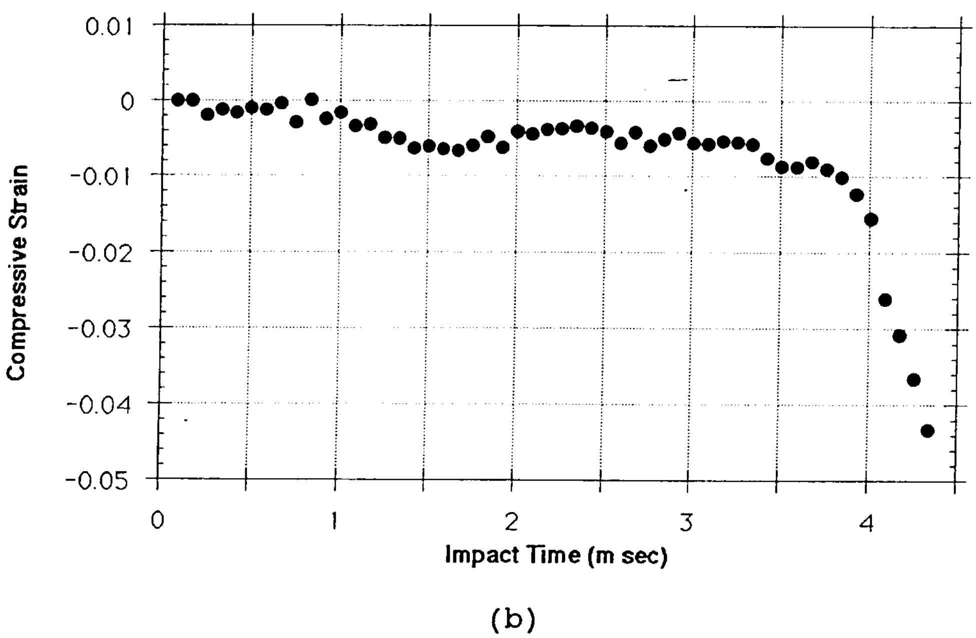

Figure 8b. Strain in the composite laminate subjected to impact.

(Figure 4b), occurs at the end of the impact event when the material failed. Figure 9 shows the stress state in the composite in terms of impact duration of about 5 ms. The maximum stress, resulting from rigid body acceleration only, of about 120 ksi, occurs at 4 ms. The corresponding compressive strain calculated from the streak film is about 1.5%. The ultimate compressive strength would be significantly higher if the stress attributable to shock wave is also taken into consideration.

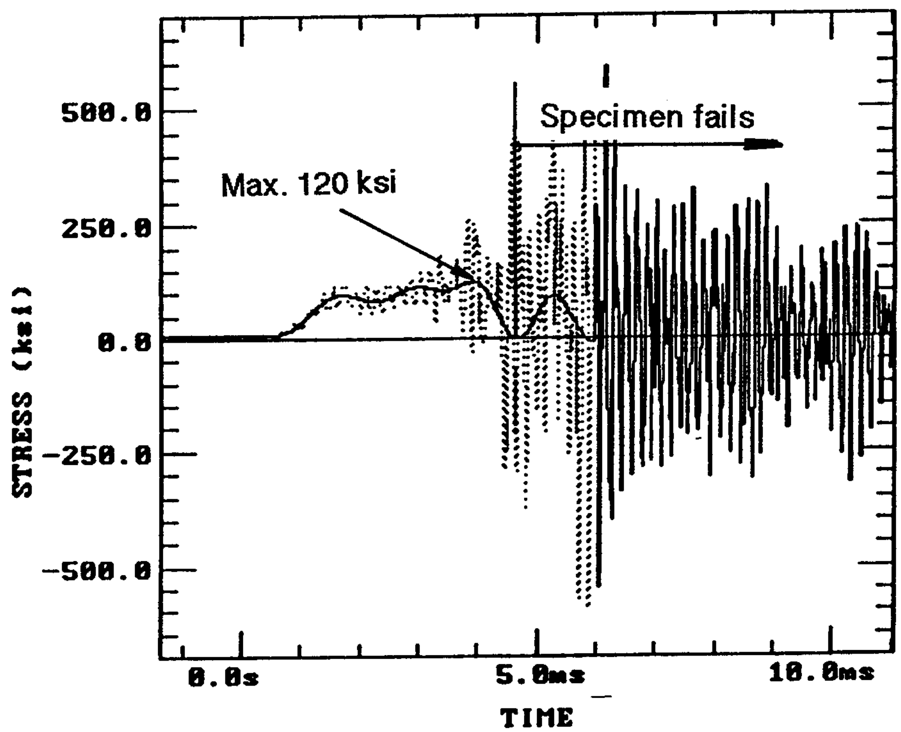

Figure 9. Stress in composite laminate subjected to impact.

Static tests using an IITRI test fixture (Adams and Odom 1991) are also performed for comparison. The ultimate strength and strain are significantly lower, measured to be 110 ksi and 1.1%, respectively. The difference is believed to be attributable to the effects of loading rate or strain rate on material strength. If the stress due to the acoustic wave is taken into consideration, dynamic effect on the behavior of material is even more significant. The source of this rate-dependant behavior is suggested by the nature of the failures observed in the composite specimens. Figure 10 shows a typical failure of specimen after an impact test. The tested specimen shows the failure is initiated by transverse delamination then followed

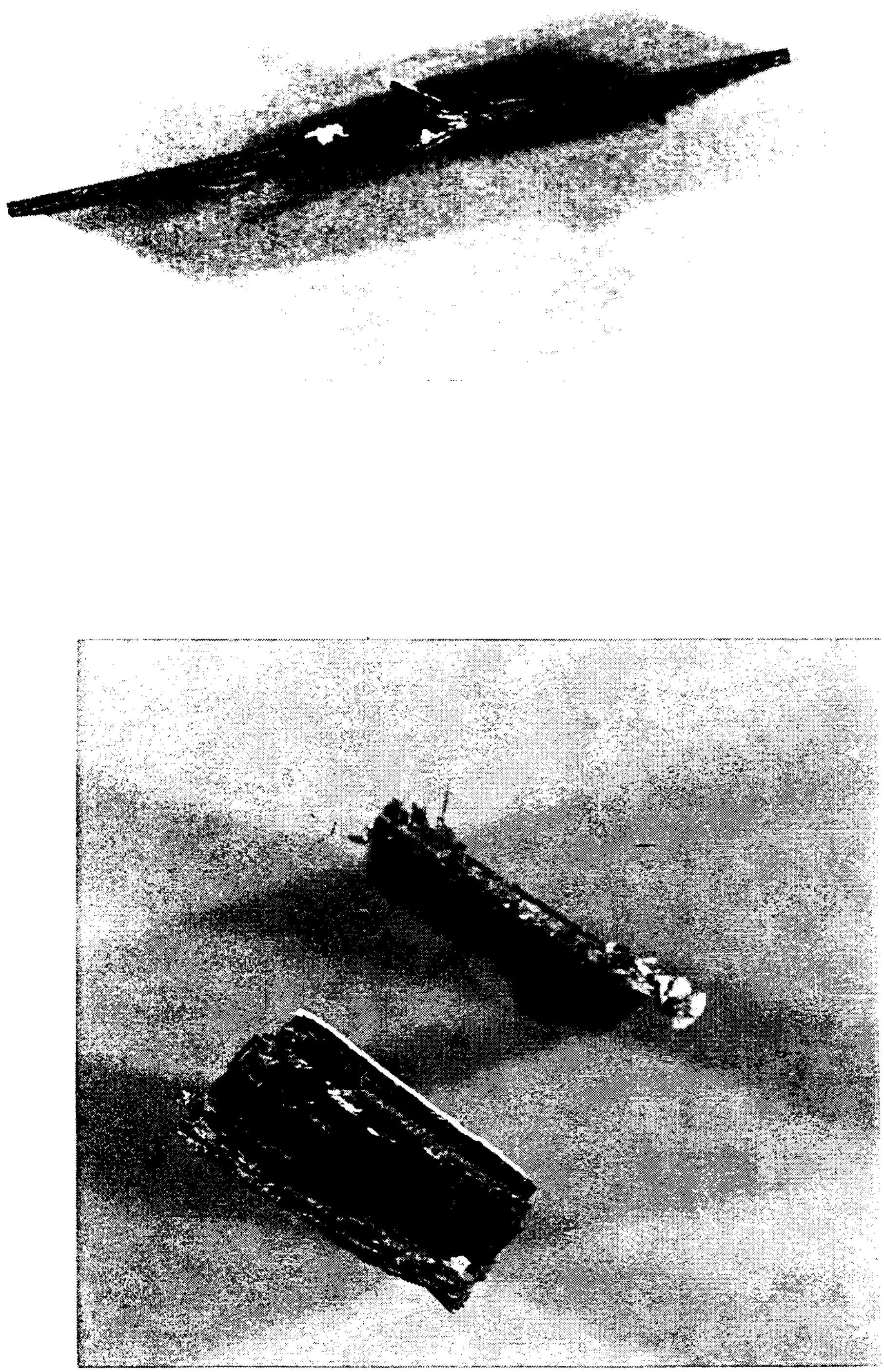

Figure 10. Specimen after impact.

by fiber buckling. Since the highly rate-dependent materials, polymer matrix materials, dominate the transverse properties of the composite, the failure strain of the composite and its dynamic strength will increase as strain and loading rates increase.

5. REDUCTION OF STRESS WAVES

The composite strength measured in the experiment described in the previous section showed the presence of high-frequency and magnitude acoustic waves. The effects of these cyclic, high-frequency, and high-amplitude stress waves on material strength are not known. It can certainly be expected that the stress waves would result in extra loads in the test specimen. However, it is believed that the stress waves exist only in the MEM since there is a significant change of cross-section area from the fixture to the MEM. Engineering effort on both theoretical and experimental aspects are performed to understand and reduce the stress waves.

To reduce the magnitude of stress waves, several ideas are examined and summarized. Both wave trapping/breaking and mechanical damping mechanisms have been investigated and the experimental setup is modified to reduce the stress waves attributable to impact. The ideas for the wave trapping and breaking mechanism are illustrated schematically in Figure 11. For the wave trapping setup, a thick piece (4 in) of glass-reinforced polyethylene disk with the same diameter of the MEM is attached to the end of the system. The intention is to absorb the reflecting stress waves at the very end of the system using a soft and high damping material. Following the similar idea, a piece of aluminum honeycomb is attached to the end of the system to break the reflecting stress waves. Both the wave trapping and breaking methods do result in some improvement in reduction of wave magnitude. However, more interfaces are created by attaching the material at the system. Accordingly, the wave patterns are more complex. This is attributed to the reflection of wave at the interface between the MEM and the wave trapping/breaking materials. This method was abandoned after a few trials.

The schematic of the mechanical damping mechanism is illustrated in Figure 12. The idea is to block and/or absorb the wave attributed to the impact flowing into the test specimen which allows the transmission of rigid body force. The idea is straightforward; however, the addition of a traditional damper into the system will, in general, change the loading rate in the test specimen. Accordingly, an iteration for a new system design is needed to obtain the desired loading rate. This procedure is very time

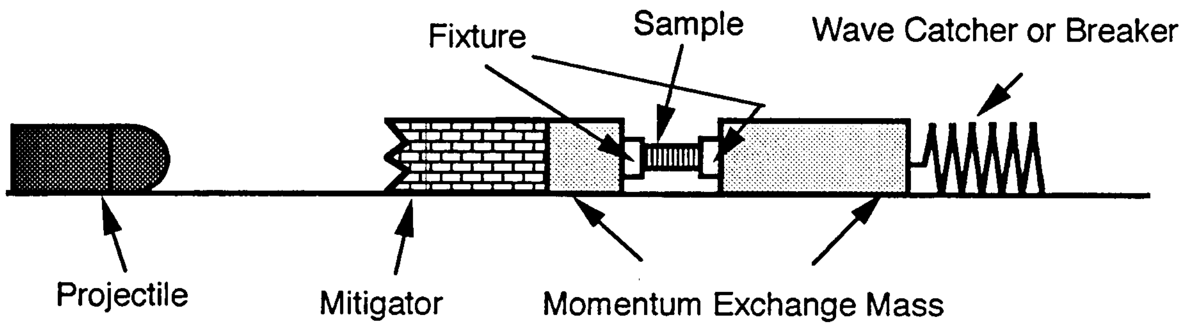

Figure 11. Wave catching and/or breaking mechanism.

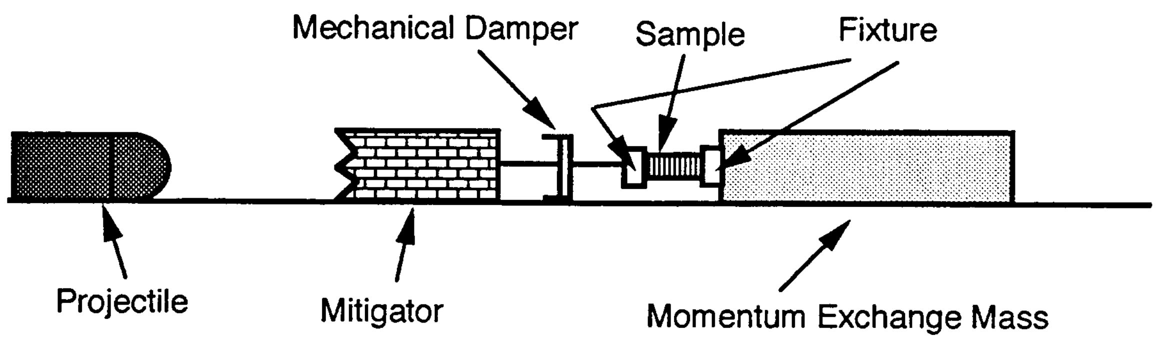

Figure 12. Experimental setup using mechanical damping mechanism.

consuming with no guarantee that the desired loading rate and wave reduction will be obtained simultaneously. Based on this understanding, a "shock snubber" filled with damping material is used to force transmission and reduce stress waves simultaneously. Test results of aluminum and composite samples are illustrated in Figures 13a and 13b, respectively. The acoustic waves are greatly reduced compared to the previous test results. The ultimate stress of aluminum is about the same level. The results indicate that the acoustic stress waves exist mainly in the MEM, as described in Section 3.2. The Fourier transform can be used to cull the rigid body acceleration (force) that causes the failure of the specimen. The composite samples have never been tested to failure using the new setup while the damage of the fixture occurs. However, at the time of this writing, the development of the experimental setup for testing material at the interior ballistic rates of loading is nearing completion.

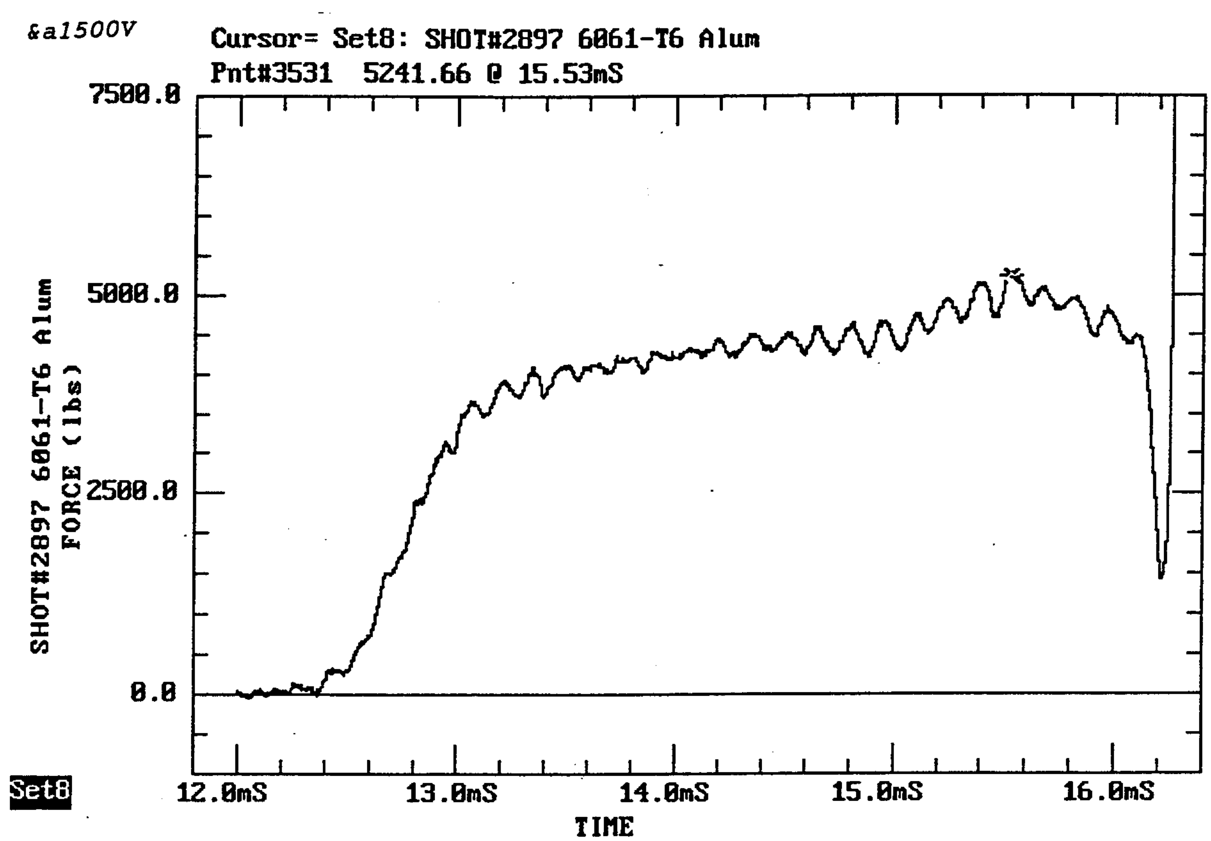

Figure 13a. Aluminum test results from the modified experimental setup.

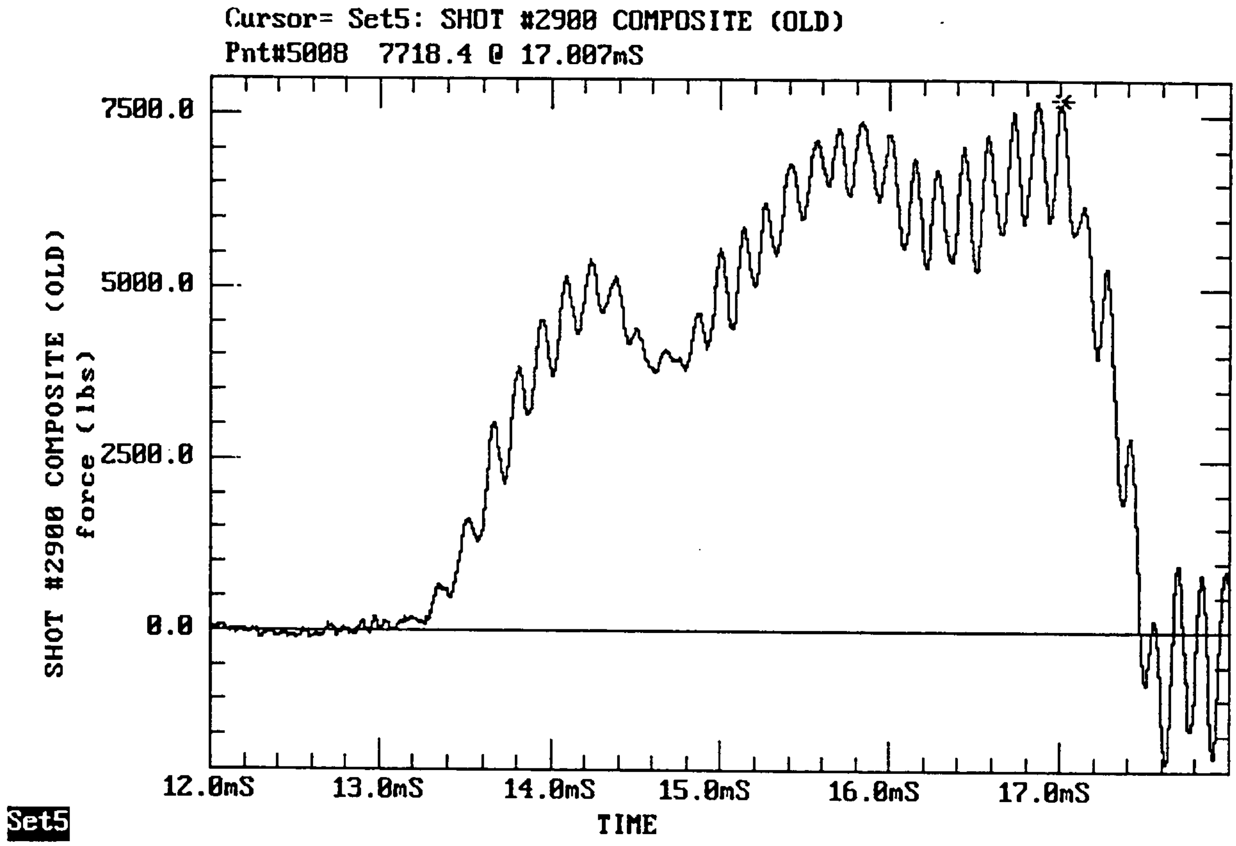

Figure 13b. Composite test results from the modified experimental setup.

6. CONCLUSIONS

An experimental method has been developed to determine the dynamic properties of composite materials experienced during the interior ballistic cycle. Airgun systems and fixtures were designed and fabricated to hold the specimen in correct alignment during impact, and to provide a uniform transfer of stress into the specimen. Data acquisition and reduction methods for determining the deformation of material were also developed and were verified in tests of aluminum samples.

Strain rate effects on the compressive properties of the composite are clearly observed. For the specific material and layup $[(0/45/-45/0)_4]$ used in the tests, a conservative estimate of at least a 10% increase of strength due to dynamic effects is observed. The data obtained from this new test method are very useful for the design and analysis of structural components subjected to ballistic-type loading conditions.

7. REFERENCES

Adams, D. F., and E. Q. Lewis. "Influence of Specimen Gauge Length and Loading Method on the Axial Compressive Strength of a Unidirectional Composite Material." Experimental Mechanics, pp. 14–20, March 1991.

Adams, D. F., and E. M. Odom. "Influence of Test Fixture Configuration on the Measured Compressive Strength of a Composite Material." Journal of Composite Technology and Research, vol. 13, no. 1, pp. 36–40, 1991.

Fourier transform analysis. "View-Point." Maxwell Laboratory, S^3 Division, La Jolla, CA, 1991.

Kolsky, H. "An Investigation of Mechanical Properties of Materials at Very High Rates of Loading." Proceedings of Physics Society, London, vol. 62B, pp. 676–700, 1949.

Maiden, C. J., and S. J. Green. "Compressive Strain-Rate Tests on Six Selected Materials at Strain Rates From 10^{-3} to 10^{-4} in/in/s." Journal of Applied Mechanics, pp. 496–504, September 1966.

Nicholas, T., and S. J. Bless. "High Strain Rate Tension Testing." Metal Tension, American Society of Metals, 9th ed., vol. 8, pp. 208–214, 1985.

Staab, G. F., and A. Gilat. "A Direct-Tension Split Hopkinson Bar for High Strain-Rate Testing." Experimental Mechanics, pp. 232–235, September 1991.

INTENTIONALLY LEFT BLANK.

NO. OF COPIES	ORGANIZATION
2	ADMINISTRATOR ATTN DTIC DDA DEFENSE TECHNICAL INFO CTR CAMERON STATION ALEXANDRIA VA 22304-6145
1	COMMANDER ATTN AMCAM US ARMY MATERIEL COMMAND 5001 EISENHOWER AVE ALEXANDRIA VA 22333-0001
1	DIRECTOR ATTN AMSRL OP SD TA US ARMY RESEARCH LAB 2800 POWDER MILL RD ADELPHI MD 20783-1145
3	DIRECTOR ATTN AMSRL OP SD TL US ARMY RESEARCH LAB 2800 POWDER MILL RD ADELPHI MD 20783-1145
1	DIRECTOR ATTN AMSRL OP SD TP US ARMY RESEARCH LAB 2800 POWDER MILL RD ADELPHI MD 20783-1145
2	COMMANDER ATTN SMCAR TDC US ARMY ARDEC PCTNY ARSNL NJ 07806-5000
1	DIRECTOR ATTN SMCAR CCB TL BENET LABORATORIES ARSENAL STREET WATERVLIET NY 12189-4050
1	DIR USA ADVANCED SYSTEMS ATTN AMSAT R NR MS 219 1 R&A OFC AMES RESEARCH CENTER MOFFETT FLD CA 94035-1000

NO. OF COPIES	ORGANIZATION
1	COMMANDER ATTN AMSMI RD CS R DOC US ARMY MISSILE COMMAND REDSTONE ARSNL AL 35898-5010
1	COMMANDER ATTN AMSTA JSK ARMOR ENG BR US ARMY TANK AUTOMOTIVE CMD WARREN MI 48397-5000
1	DIRECTOR ATTN ATRC WSR USA TRADOC ANALYSIS CMD WSMR NM 88002-5502
1	COMMANDANT ATTN ATSH CD SECURITY MGR US ARMY INFANTRY SCHOOL FT BENNING GA 31905-5660

ABERDEEN PROVING GROUND

NO. OF COPIES	ORGANIZATION
2	DIR USAMSAA ATTN AMXSY D AMXSY MP H COHEN
1	CDR USATECOM ATTN AMSTE TC
1	DIR USAERDEC ATTN SCBRD RT
1	CDR USACBDCOM ATTN AMSCB CII
1	DIR USARL ATTN AMSRL SL I
5	DIR USARL ATTN AMSRL OP AP L

NO. OF COPIES | ORGANIZATION

11 DIRECTOR
ATTN SMCAR CCB
F HEIZER
J KEANE
T ALLEN
J VASILAKIS
G FRIAR
J ZWEIG
T SIMKINS
V MONTVORI
J WRZOCHALSKI
G D'ANDREA
R HASENBEIN
BENET LABORATORIES
WATERVLIET NY 12189-4050

1 COMMANDER
ATTN SMCWV QAE Q C HOWARD
WATERVLIET ARSENAL
WATERVLIET NY 12189-4050

1 COMMANDER
ATTN SMCWV SPM T MCCLOSKEY
WATERVLIET ARSENAL
WATERVLIET NY 12189-4050

9 COMMANDER
ATTN SMCAR CCH T
S MUSALLI
P CHRISTIAN
K FEHSAL
N KRASNOW
R CARR
SMCAR CCH V E FENNELL
SMCAR CCHP J LUTZ
SMCAR CCH J DELORENZO
SMCAR CC J HEDDERICH
PCTNNY ARSNL NJ 07806-5000

3 COMMANDER
ATTN SMCAR TD
R PRICE
V LINDER
T DAVIDSON
PCTNNY ARSNL NJ 07806-5000

1 COMMANDER
ATTN AMSMC PBM K
PROD BASE MODERNIZATION ACTIVITY
PCTNNY ARSNL NJ 07806-5000

NO. OF COPIES | ORGANIZATION

1 COMMANDER
ATTN STRBE JBC C KOMINOS
US ARMY BELVOIR RD&E CENTER
FORT BELVOIR VA 22060-5606

2 COMMANDER
ATTN AMSMI RD W MCCORKLE
AMSMI RD ST P DOYLE
US ARMY MISSILE COMMAND
REDSTONE ARSENAL AL 35898

3 COMMANDER
ATTN SMCAR FSA M
R BOTTICELLI
F DIORIO
SMCAR FSA
C SPINELLI
PCTNNY ARSNL NJ 07806-5000

3 PROJECT MANAGER
ATTN COL NAPOLIELLO
LTC A ELLIS
G DELCOCO
PCTNNY ARSNL NJ 07806-5000

1 COMMANDER
ATTN SMCWV QA QS K INSCO
WATERVLIET ARSENAL
WATERVLIET NY 12189-4050

2 PROJECT MANAGER
SADARM
PCTNNY ARSNL NJ 07806-5000

7 PROJECT MANAGER
ATTN SFAE AR TMA
COL HARTLINE
C KIMKER
SFAE AR TMA MD
H YUEN
J MCGREEN
SFAE AR TMA ME
R JOINSON
D GUZOWITZ
SFAE AR TMA MP
W LANG
PCTNNY ARSNL NJ 07806-5000

NO. OF COPIES	ORGANIZATION
1	US ARMY RESEARCH LABORATORY ATTN AMSRL CP CA D SNIDER 2800 POWDER MILL RD ADVANCED CONCEPTS AND PLANS ADELPHI MD 20783
1	US ARMY MATERIEL COMMAND ATTN AMCDCG T R CHAIT 5001 EISENHOWER AVE ALEXANDRIA VA 22333-0001
2	PEO ARMAMENTS ATTN SFAE AR PM D ADAMS T MCWILLIAMS PCTNNY ARSNL NJ 07806-5000
2	US ARMY RESEARCH OFFICE ATTN ANDREW CROWSON AMXRO MCS J CHANDRA PO BOX 12211 RSRCH TRNGL PK NC 27709-2211
2	NASA LANGLEY RESEARCH CENTER ATTN F BARTLETT JR AMSRL VS W ELBER MAIL STOP 266 HAMPTON VA 23681-0001
1	COMMANDER ATTN AFWAML R KIM WRIGHT PATTERSON AIR FORCE BASE DAYTON OH 45433
2	COMMANDER ATTN J KELLY B WILCOX 3701 N FAIRFAX DR ARLINGTON VA 22203-1714
6	DIRECTOR USARL ATTN AMSRL MA P L JOHNSON B HALPIN T CHOU AMSRL MA PA D GRANVILLE W HASKELL AMSRL MA MA G HAGNAUER WATERTOWN MA 02172-0001

NO. OF COPIES	ORGANIZATION
9	DIRECTOR USARL ATTN AMSRL WT PD (ALC) A ABRAHAMIAN K BARNES M BERMAN H DAVISON A FRYDMAN T LI W MCINTOSH E SZYMANSKI H WATKINS 2800 POWDER MILL RD ADELPHI MD 20783-1145
1	NAVAL RESEARCH LABORATORY ATTN I WOLOCK CODE 6383 WASHINGTON DC 20375-5000
1	OFFICE OF NAVAL RESEARCH ATTN YAPA RAJAPAKSE MECH DIV CODE 1132SM ARLINGTON VA 22217
2	DAVID TAYLOR RESEARCH CENTER ATTN R ROCKWELL W PHYILLAIER BETHESDA MD 20054-5000
1	DAVID TAYLOR RESEARCH CENTER ATTN J CORRADO CODE 1702 SHIP STRUCTURES AND PROTECTION DEPT BETHESDA MD 20084
4	DIRECTOR ATTN R CHRISTENSEN S DETERESA W FENG F MAGNESS PO BOX 808 LIVERMORE CA 94550
2	PACIFIC NORTHWEST LABORATORY ATTN M SMITH M GARNICH PO BOX 999 RICHLAND WA 99352

NO. OF COPIES	ORGANIZATION
6	DIRECTOR ATTN C ROBINSON G BENEDETTI W KAWAHARA K PERANO D DAWSON P NIELAN PO BOX 969 LIVERMORE CA 94550-0096
1	DIRECTOR ATTN D RABERN MEE 13 MAIL STOP J 576 PO BOX 1633 LOS ALAMOS NM 87545
2	VA POLYTECHNICAL INST & STATE U ATTN MICHAEL W HYER KENNETH L REIFSNIDER BLACKSBURG VA 24061-0219
2	UNIVERSITY OF DAYTON RSRCH INSTITUTE ATTN RAN Y KIM AJIT K ROY 300 COLLEGE PARK AVE DAYTON OH 45469-0168
1	DREXEL UNIVERSITY ATTN ALBERT S D WANG 32ND AND CHESTNUT ST PHILADELPHIA PA 19104
1	UNIVERSITY OF DAYTON ATTN JAMES M WHITNEY 300 COLLEGE PARK AVE DAYTON OH 45469-0240
1	PURDUE UNIVERSITY ATTN C T SUN SCHOOL OF AERO AND ASTRO W LAFAYETTE IN 47907-1282
1	UNIVERSITY OF KENTUCKY ATTN LYNN PENN 763 ANDERSON HALL LEXINGTON KY 40506-0046

NO. OF COPIES	ORGANIZATION
3	UNIVERSITY OF DELAWARE ATTN J GILLESPE B PIPES M SANTARE 201 SPENCER LABORATORY NEWARK DE 19716
2	NORTH CAROLINA STATE UNIVERSITY ATTN W RASDORF L SPAINHOUR PO BOX 7908 RALEIGH NC 27696-7908
1	UNIVERSITY OF UTAH ATTN S SWANSON DEPT OF MECHANICAL AND INDSTRL ENGINEERING SALT LAKE CITY UT 84112
1	STANFORD UNIVERSITY ATTN S TSAI DEPT OF AERONAUTICS AND AEROBALLISTICS DURANT BLDG STANFORD CA 94305
1	PENNSYLVANIA STATE UNIVERSITY ATTN RENATA S ENGEL 245 HAMMOND BLDG UNIVERSITY PARK PA 16801
1	PENNSYLVANIA STATE UNIVERSITY ATTN DAVID W JENSEN 223 N HAMMOND UNIVERSITY PARK PA 16802
1	PENNSYLVANIA STATE UNIVERSITY ATTN RICHARD MCNITT 227 HAMMOND BLDG UNIVERSITY PARK PA 16802
1	UCLA ATTN H THOMAS HAHN MANE DEPT ENGRG IV LOS ANGELES CA 90024-1597
1	UNIV OF IL AT URBANA-CHAMPAIGN ATTN J ECONOMY 104 S WRIGHT ST 216 TALBOT LABORATORY URBANA IL 61801

NO. OF COPIES	ORGANIZATION
1	VA POLYTECHNIC INST & STATE U ATTN M W HYER ENGNRG SCIENCE AND MECH DEPT BLACKSBURG VA 24061-0219
2	OLIN CORPORATION ATTN E STEINER B STEWART PO BOX 127 RED LION PA 17356
1	CHAMBERLAIN MFG CORP ATTN T LYNCH 550 ESTHER ST WATERLOO IA 50704
1	OLIN CORPORATION ATTN L WHITMORE 10101 9TH ST N ST PETERSBURG FL 33702
3	ALLIANT TECHSYSTEMS INC ATTN C CANDLAND J BODE K WARD 5640 SMETANA DR MINNETONKA MN 55343
1	ALLIANT TECHSYSTEMS INC PRECISION ARMAMENTS SYSTEMS GROUP 7225 NORTHLAND DR BROOKLYN PARK MN 55428
1	VA POLYTECHNIC INST & STATE U ATTN M W HYER ENGNRG SCIENCE AND MECH DEPT BLACKSBURG VA 24061-0219
1	CUSTOM ANALYTICAL ENGNRG SYS INC ATTN A ALEXANDER STAR RTE BOX 4A FLINTSTONE MD 21530
2	INSTITUTE FOR ADVANCED TECHNOLOGY ATTN T KIEHNE H FAIR 4030 2 W BRAKER LN AUSTIN TX 78759

NO. OF COPIES	ORGANIZATION
2	KAMAN SCIENCES CORPORATION ATTN D ELDER J BETZ PO BOX 7463 COLORADO SPRINGS CO 80933
3	LORAL/VOUGHT SYSTEMS ATTN G JACKSON K COOK L L HADDEN 1701 W MARSHALL DR GRAND PRAIRIE TX 75051
1	INTERFEROMETRICS INC ATTN R LARRIVA VICE PRESIDENT 8150 LEESBURG PIKE VIENNA VA 22100
1	ARMTEC DEFENSE PRODUCTS ATTN STEVE DYER 85 901 AVE 53 PO BOX 848 COACHELLA CA 92236

ABERDEEN PROVING GROUND

NO. OF COPIES	ORGANIZATION
18	Dir, USARL ATTN: AMSRL-SL-B, P. Deitz AMSRL-SL-I, D. Haskell AMSRL-SL-BA, J. Walbert AMSRL-SL-BL, D. Bely AMSRL-CI-CB, R. Kaste AMSRL-CI-C, W. Sturek AMSRL-CI-S, A. Mark AMSRL-WT-W, C. Murphy AMSRL-WT-WC, J. Rocchio AMSRL-WT-WA, H. Rogers B. Moore A. Baran AMSRL-WT-WB, F. Brandon W. D'Amico AMSRL-WT-WE, J. Temperley AMSRL-WT-T, W. Morrison AMSRL-WT-TA, W. Gillich W. Bruchey

NO. OF COPIES	ORGANIZATION
29	Dir, USARL ATTN: AMSRL-WT-TC, K. Kimsey R. Coates W. de Rosset AMSRL-WT-TD, D. Dietrich G. Randers-Pehrson J. Huffington A. Das Gupta J. Santiago AMSRL-WT-P, A. Horst AMSRL-WT-PA, T. Minor C. Leveritt D. Kooker AMSRL-WT-PB, E. Schmidt P. Plostins AMSRL-WT-PC, R. Fifer AMSRL-WT-PD, B. Burns W. Drysdale K. Bannister T. Bogetti J. Bender R. Murray R. Kirkendall T. Erline D. Hopkins S. Wilkerson D. Henry R. Kaste L. Burton J. Tzeng

USER EVALUATION SHEET/CHANGE OF ADDRESS

This Laboratory undertakes a continuing effort to improve the quality of the reports it publishes. Your comments/answers to the items/questions below will aid us in our efforts.

1. ARL Report Number ARL-TR-696 Date of Report February 1995

2. Date Report Received ________

3. Does this report satisfy a need? (Comment on purpose, related project, or other area of interest for which the report will be used.) ________

4. Specifically, how is the report being used? (Information source, design data, procedure, source of ideas, etc.) ________

5. Has the information in this report led to any quantitative savings as far as man-hours or dollars saved, operating costs avoided, or efficiencies achieved, etc? If so, please elaborate. ________

6. General Comments. What do you think should be changed to improve future reports? (Indicate changes to organization, technical content, format, etc.) ________

CURRENT ADDRESS

Organization

Name

Street or P.O. Box No.

City, State, Zip Code

7. If indicating a Change of Address or Address Correction, please provide the Current or Correct address above and the Old or Incorrect address below.

OLD ADDRESS

Organization

Name

Street or P.O. Box No.

City, State, Zip Code

(Remove this sheet, fold as indicated, tape closed, and mail.)

(DO NOT STAPLE)

DEPARTMENT OF THE ARMY

OFFICIAL BUSINESS

NO POSTAGE NECESSARY IF MAILED IN THE UNITED STATES

BUSINESS REPLY MAIL
FIRST CLASS PERMIT NO 0001, APG, MD

Postage will be paid by addressee

Director
U.S. Army Research Laboratory
ATTN: AMSRL-OP-AP-L
Aberdeen Proving Ground, MD 21005-5066